AD-A125 953 HIGH-POWER GENERATION OF MICROWAVE AND INFRARED RADIATION(U) MITRE CORP MCLEAN VA H D ABARBANEL ET AL. FEB 83 JSR-82-975

1/1

UNCLASSIFIED

F/G 20/8 NL

END

FILMED

DTIC

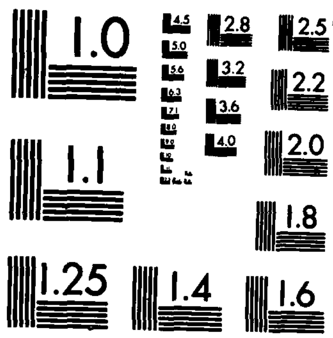

MICROCOPY RESOLUTION TEST CHART
NATIONAL BUREAU OF STANDARDS-1963-A

High-Power Generation of Microwave and Infrared Radiation

MITRE

High-Power Generation of Microwave and Infrared Radiation

H.D.I. Abarbanel

J. M. Cornwall

February 1983

JSR-82-975

JASON
The MITRE Corporation
1820 Dolley Madison Boulevard
McLean, Virginia 22102

TABLE OF CONTENTS

A

LIST OF ILLUSTRATIONS

HIGH-POWER GENERATION OF ELECTROMAGNETIC RADIATION
WITH FREQUENCIES 10-10^5 GHz BY
RELATIVISTIC ELECTRON BEAM-COLD PLASMA INTERACTIONS

1.0 INTRODUCTION

The work reported here is a JASON IR&D project. It began when the authors attended a talk by Professor Gregory Benford, of the University of California at Irvine, on experimental simulation of high-energy astrophysical processes. It seemed to us that the experimental device described by Benford--which directs a relativistic electron beam into a plasma--might be modified to become a high-power (order of gigawatts) generator usable from microwave frequencies up to the IR region. The prospects are that such a generator could have reasonable wall-plug efficiency, along with a size and weight compatible with some mobility. → p5

Standard theories of weak beam-plasma interaction predict that the electromagnetic radiation in this beam-plasma collision would be dominantly at the oscillation frequency of the plasma: $\omega_p = (4\pi n_o e^2/m)^{1/2}$ and, from nonlinear interactions, at a few harmonics $\omega = n\omega_p$, n = 2 or 3 [see, e.g., Kaplan and Tsytovich (1973)]. A typical plasma density in the Irvine apparatus is $n_o \sim 10^{13}/cm^3$, which gives $\frac{\omega_p}{2\pi} \approx 30$ GHz . So one would expect to see a peak near 30 GHz and perhaps also at 60 GHz in the Irvine

experiments. In fact, their measured power spectra are broad band with significant signal strength all the way to 120 GHz which is the current upper limit for the detectors used by the Irvine group. The spectra show no signs of falling off even there.

An important feature of the Irvine device is that the relativistic beam plasma density is a finite fraction (3-10%) of the density of the plasma into which the beam is injected. This appears to be essential for the generation of broad-band high-frequency radiation. When the beam density is lowered so that it is truly a small fraction of the stationary plasma density, the Irvine group does see lines at ω_p and $2\,\omega_p$, as expected from the conventional theories of weak beam-plasma turbulence, and a greatly reduced total wave intensity. But as the beam density is increased these features fall away to be replaced by the apparent broad-band spectrum we noted above, with very high power levels. No signs are visible of spectral lines developing at $3\,\omega_p$, $4\,\omega_p$, . . . as the broad band phenomenon sets in.

It appears then that the conventional process of two Langmuir waves of frequency ω_p interacting nonlinearly to produce a new electromagnetic wave at $2\,\omega_p$ is swamped in the Irvine experiment by another mechanism. Benford suggests that this is a "Comptonization" of the Langmuir waves through their being scattered

by the relativistic electrons to produce electromagnetic radiation at frequencies up to $\sim (1 - v/c)^{-1}\ \omega_p$, or $\approx 20\ \omega_p$ in the Irvine device. This phenomenon could only become important when the intensity of the relativistic electron beam is a finite fraction of n_o , the baackground plasma density. Only then would there be sufficient available power to drive the photon frequency boosting process--which is inherently a weak process--strongly enough to produce visible power at the frequencies observed.

Benford's current device, which is designed only to explore astrophysical processes and not to be an efficient generator, emits high intensity broadband radiation (typically 1-10 MW/GHz) into an angular cone of some 15^o width. The total energy radiated in photons per 100 nsec beam pulse is ~ 100 J, at a wall-plug efficiency of 0.1%. The measured frequency spectrum is from ~ 10 GHz to > 120 GHz (the upper limit of the instruments), and shows no sign of turning over at the upper-limit frequency. These numbers are already interesting when compared to the state of the art in the upper frequency ranges, and it may well be that the efficiency can be materially raised at the same time that the bandwidth and angular spread are reduced.

It is instructive to compare this device to a free-electron laser (FEL), since the kinematics of high-frequency photon

generation by relativistic electrons (i.e., Comptonization) are quite analogous in the two devices. Just as in the FEL, the output photon frequency varies as $\gamma^2 = (1-v^2/c^2)^{-1}$. Benford's device at present uses 1-MeV electrons $(\gamma \simeq 3)$, which (see below) yields a theoretical upper-limit frequency of the order of 300 GHz. Thus the present machine with 5 MeV electrons $(\gamma \simeq 11)$ could reach frequencies of the order of 4×10^{11} Hz and a redesigned machine, which we describe later, could in principle reach to $\gtrsim 10^{14}$ Hz (wavelength $\simeq 3\mu$) even with 1 MeV electrons. These frequencies, for a given γ , are considerably higher than can be gotten from a conventional FEL, and the explanation is that the wavelength of the wiggler in the modified plasma machine can be made much smaller than the usual mechanical wiggler of an FEL. This is because the "wiggler" is a plasma wave instead of a solid helical magnet. The price paid for this shorter wavelength is reduced control over the precise features of the wiggler, since it will have a spread of wavelengths and angular orientations. It is therefore more difficult to control the wavelength and angular spread of the emitted radiation, but there are possibilities for running the device as a multi-mode oscillator or even as a true laser by putting it in a resonant cavity.

The present Benford device uses a single relativistic electron beam both to set up the plasma-wave wiggler (via a

two-stream instability) and to radiate high-frequency photons as in an FEL. The single-beam setup is used to simulate various astrophysical processes, but it is not the best way to make a high-power oscillator. In this report we suggest that two beams be used, roughly oppositely directed, and both interacting with a stationary plasma. The second beam is of substantially slower velocity and can be either electrons or ions; its role is to set up the wiggler which then stimulates the relativistic electrons to radiate. Using a second, oppositely-directed, beam greatly improves the kinematic control of photon emission, allowing both for higher frequencies and narrower angular spread of the radiation. The extra equipment necessary to generate the second beam does not appear to add excessive size, weight, or power requirements. We also discuss tactics for modulating the second beam so as to emphasize a narrow range of wiggler wavelengths, and mention possibilities for improving efficiency.

Assuming that such improvements on the original Benford device work as intended, the question then is: What applications are there? We do not address this issue in any detail here. In fact, one of the major reasons for issuing this report is to stimulate thinking about the question of applications. We are convinced that the analysis of data from future plasma FEL's will

suggest the applications even more convincingly than one can on the basis of the present sparse experimentation.

2.0 DESCRIPTION OF THE BENFORD DEVICE

The following is based on unpublished material furni ed to us by Professor Benford, who is currently preparing some pap to be submitted for publication. An earlier version of the app us and some results are found in Benford et al. (1980).

Fig. 1 shows the present setup: A Marx generator produces a relativistic electron beam with energy $\approx$ 1 MeV, density $\approx 10^{12}$ cm^{-3}, current $\approx$ 100 kA, and pulse duration $\approx$ 100 nsec (total energy in one pulse of 10 kJ) which is shot into a background plasma of energy $\approx$ 5 eV and density 10^{12} - 10^{14} cm^{-3}. There is no applied magnetic field, although beam-generated fields reach a few hundred Gauss (profile shown at the top of Fig. 1). Thus the electron cyclotron frequency is less than 1 GHz, well below the frequencies of interest. The plasma into which the beam is injected is homogeneous to within 20% out to half the radius of the drift tube, and has only a small percentage of neutrals (so the background plasma density does not change much when the beam is injected). The plasma diagnostics consist of a microwave interferometer and calibrated diodes which are useful to an upper limit of 120 GHz.

The Marx generator is, of course, a weighty and bulky apparatus which could hardly lend itself to applications. It is

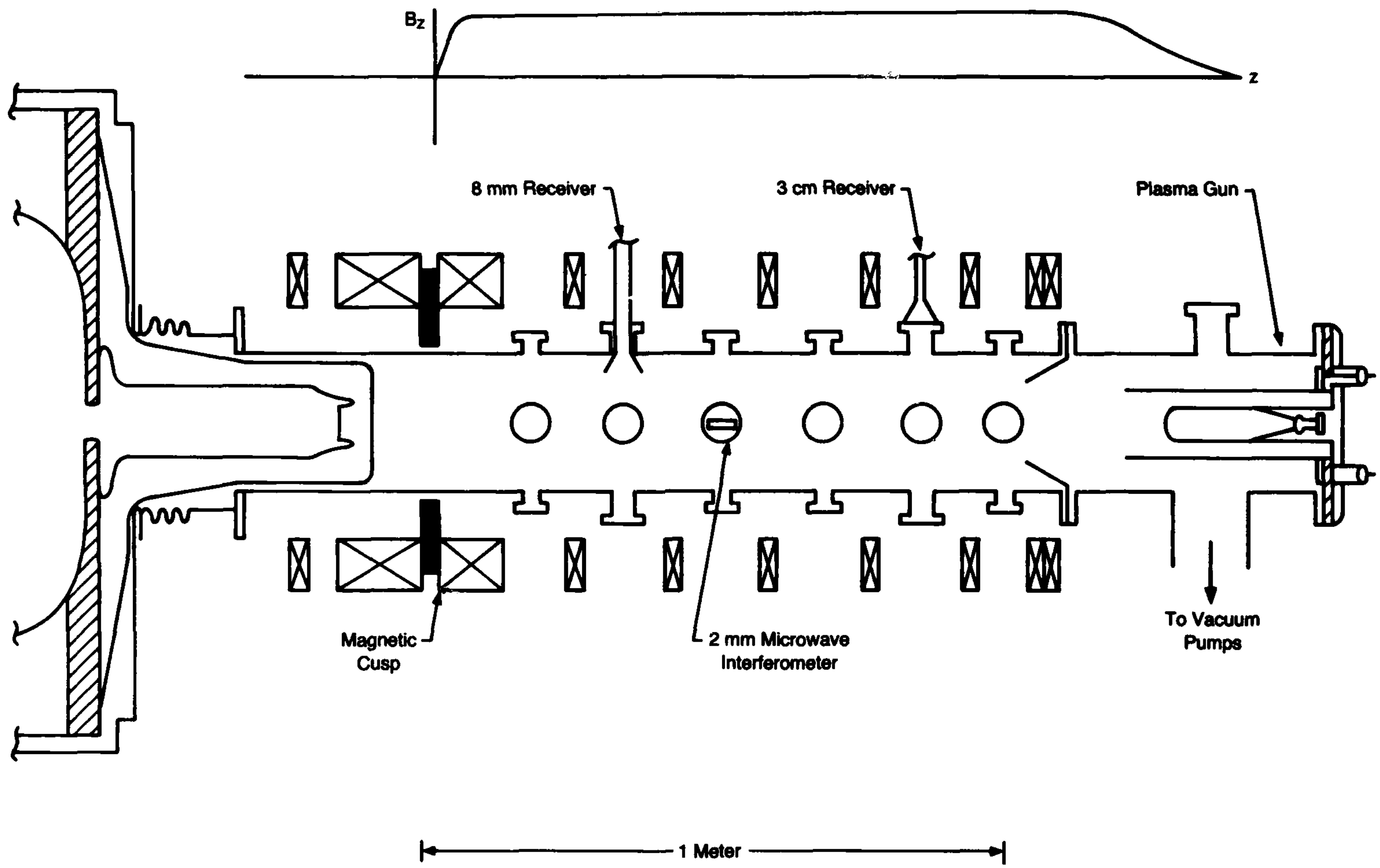

Figure 1. The Benford microwave generator.

used as the electron-beam source only because it has a fast (~ 10 nsec) rise time. But such a fast rise time appears to be entirely unnecessary for operation of the device, according to Benford, and a much smaller capacitive storage device to generate the beam would work just as well for a high-power microwave generator. Such a proposed beam source is the basis of Benford's claim that the microwave generator could be fit inside a Volkswagen.

Fig. 2 shows a typical microwave power spectrum. The beam density n_b is 10^{12} cm^{-3}, and the background plasma density n_p is 1.2×10^{13} cm^{-3} ($\omega_p/2\pi$ = 31.4 GHz) . The gaps in the power spectrum at 40-60 and 75-95 GHz are not real; they correspond to overlapping orders in the microwave spectrometer where the data points are ambiguous and have not been plotted. The vertical bars at each frequency indicate the shot-to-shot variability, which is roughly a factor of three. Note that there is no particular structure at harmonics of $\omega_p/2\pi$, and that there is no falloff at the highest measured frequency. Typical powers are 1-10 MW/GHz. At lower plasma densities it is possible to observe broadband power at up to 30 times the plasma frequency. In Fig. 2, the total emitted power is a few hundred MW, about 10^{-3} of the beam power.

Without presenting the voluminous data available, we summarize other cogent facts: The total radiated power varies

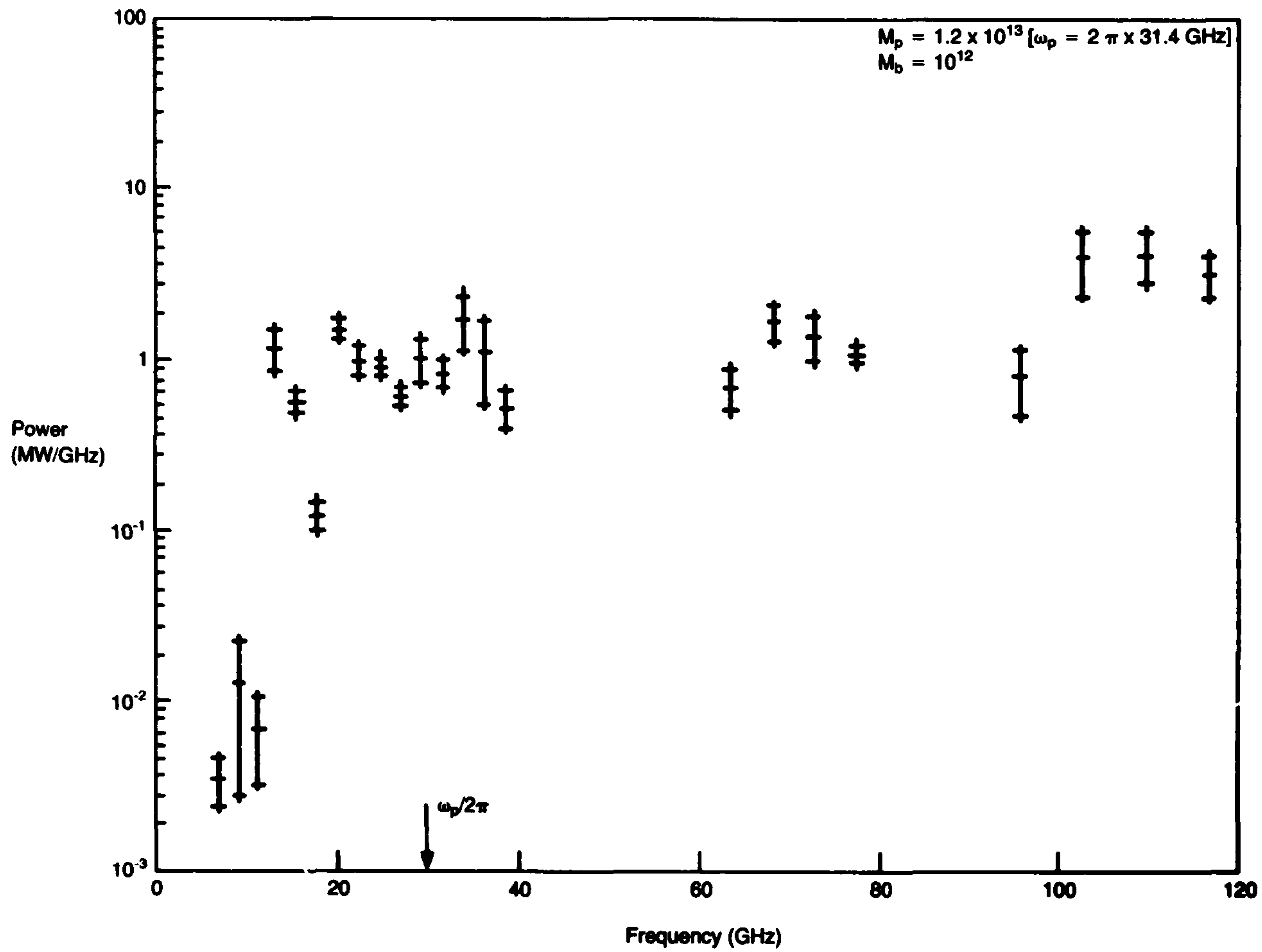

Figure 2. One of Benford's experimental power spectra. Gaps at 40-60 and 75-95 GHz are instrumental.

roughly as n_b^2 , and is roughly 10^6 times what would be expected from single-particle (i.e., incoherent) Comptonization radiation. Also, the total power is not strongly dependent either on the beam energy or on the background plasma density, although it increases as the density increases. These facts require an explanation based on partial coherence of the emission mechanism.

Of special interest for applications is the angular distribution of the microwaves. A typical example is shown in Fig. 3. The peak at $\theta \approx 75^{\circ}$ corresponds to a cone with half-angle $\approx 15^{\circ}$ from the direction of motion of the relativistic electrons. Some of the radiation shown in the figure has been reflected (e.g., from the steel chamber walls) but the general picture is that the primary emission is in a cone of some 15° width, with peak power occurring off-axis.

As currently configured, then, the Benford device achieves broad-band high-power microwave generation at frequencies which are believed (see next section) to extend to hundreds of GHz. The angular distribution is also fairly broad, and the wall-plug efficiency is of the order of 0.1%. Even though no special effort has been made to operate the device as an efficient, well-collimated microwave generator, these numbers are sufficiently interesting to consider modifications designed to improve efficiency, angular

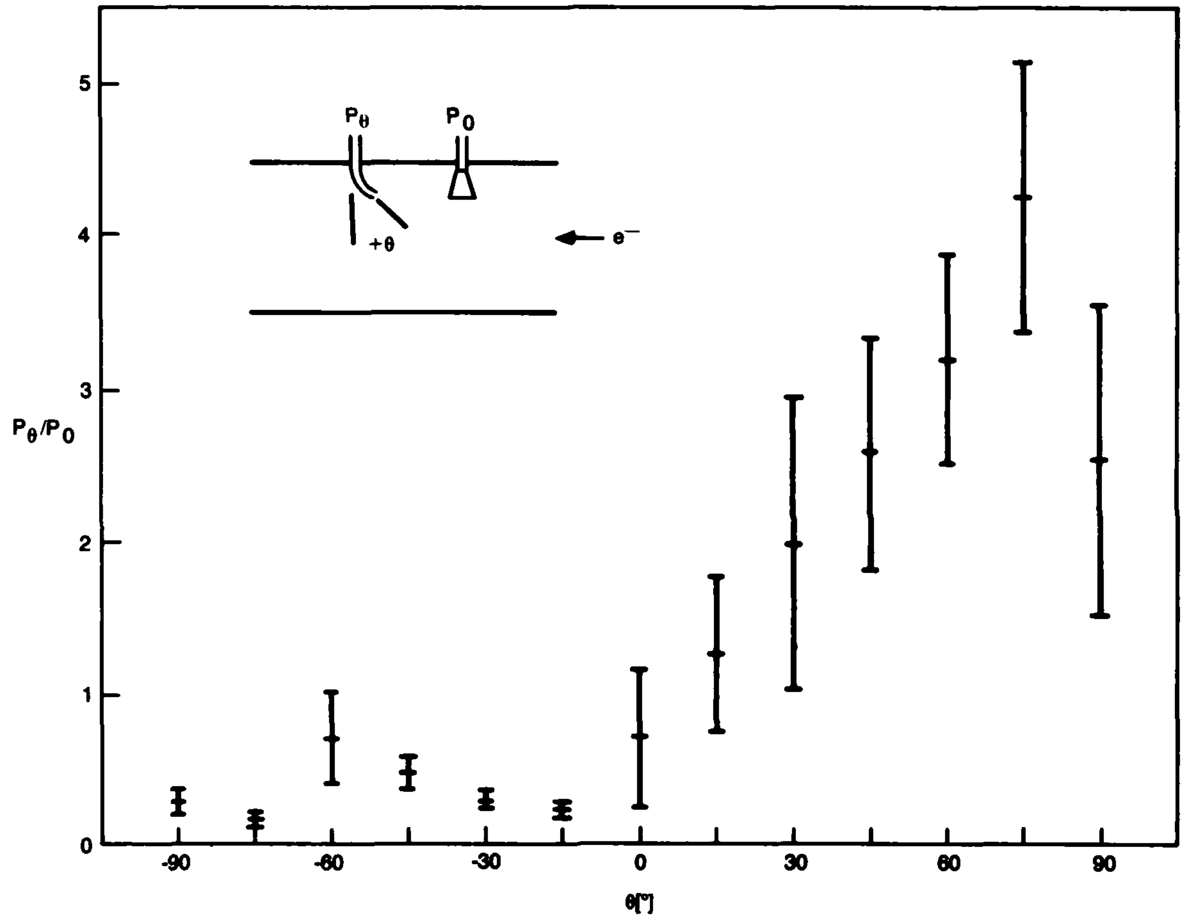

Figure 3. Angular distribution of microwave power. $\theta = 90°$ corresponds to radiation emitted along the electron beam direction.

spread, and the like. We return to such modifications after discussing theory of the device next.

3.0 THEORETICAL CONSIDERATIONS

The theory of this machine is presently rather rudimentary, and needs further development (guided by a new set of experiments). In brief, the relativistic beam drives an instability which sets up electrostatic Langmuir waves at $\omega \simeq \omega_p$, traveling in the same direction as the beam, and with a phase velocity close to that of the beam. These waves set up an electrostatic "wiggler" (as for an FEL) of wavenumber $k \simeq \omega_p v_b^{-1}$ ($v_b \simeq c$ is the beam velocity) in a growth time (according to linear theory) of

$$T_{GROWTH} \simeq (2/\sqrt{3}\ \omega_p)(2n_p/n_b)^{1/3} \tag{1}$$

which is of order a few tens of picoseconds in the Irvine apparatus. Note that $k\lambda_D \ll 1$ as long as the background plasma is non-relativistic. The beam lasts for ~ 100 nsec, so the beam-driven instability goes far into the non-linear regime and saturates, presumably by trapping. In this case, equating the trapping frequency ω_T (given by $\omega_T^2 = eE_L k m^{-1}$, where E_L is the saturation field strength of Langmuir waves) to the growth rate yields the following ratio of wave energy to relativistic beam energy:

$$\frac{E_L^2}{4\pi n_b mc^2\gamma} = \frac{9}{16}\left(\frac{n_b}{16\gamma^7 n_p}\right)^{1/3} \tag{2}$$

This is of the order 0.01 for parameters given in the last section, and gives $E_L \sim 10^6$ v/cm .

The next stage is that the relativistic electrons scatter from the Langmuir waves, converting that wave into a photon. This process of Comptonization is equally-well described as interaction of the electron with a traveling electrostatic wiggler, in FEL terms. Just as in the FEL, the crucial point is that the photon emission process is highly coherent. It is not, however, as coherent as that produced by a mechanical (magnetic) wiggler because there is inevitably a spread in both magnitude and direction for the wave numbers of the electrostatic wiggler, In the present beam-plasma device the effects of this spread are unfortunately exaggerated by the geometry of the device, in which the wiggler travels in nearly the same direction as the beam. In view of the modification of the device which we propose in the next section, we now discuss the Comptonization kinematics for a general geometry.

Let the electrostatic plasma have frequency and wave number $(\underset{\sim}{\omega}, \underset{\sim}{k})$ and the photon is described by $(\underset{\sim}{\omega}', \underset{\sim}{k}')$ with $\omega' = (\omega_p^2 + k'^2c^2)^{1/2} \simeq k'c$ (see Fig. 4). The relativistic electron has momentum $\underset{\sim}{p}$, and the angle between $\underset{\sim}{p}$ and $\underset{\sim}{k}$ is θ , between $\underset{\sim}{p}$ and $\underset{\sim}{k}'$ is θ' . The frequency-matching condition $\omega - \underset{\sim}{k}\cdot\underset{\sim}{v} = \omega' - \underset{\sim}{k}'\cdot\underset{\sim}{v}$ becomes, with $|\underset{\sim}{k}'| \simeq \omega' c^{-1}$,

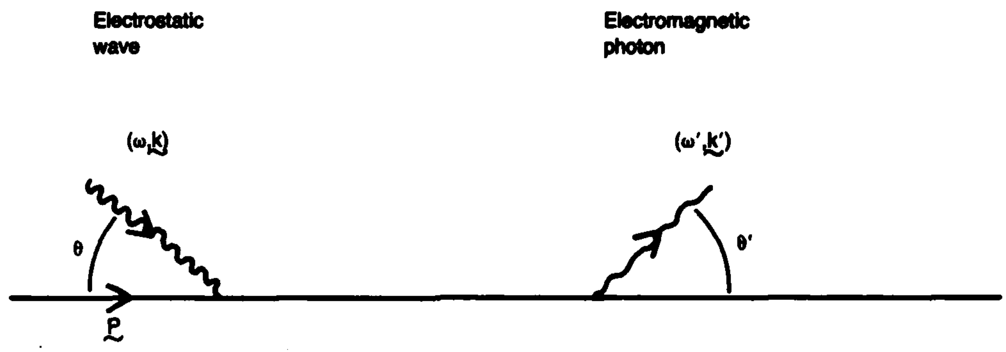

Figure 4. Compton-boosting kinematics.

$$\omega' = \frac{\omega - kv_b \cos\theta}{1-\beta\cos\theta'}, \quad \beta \equiv v_b c^{-1} \tag{3}$$

For small θ' and $\beta \approx 1$ this becomes

$$\omega' = \frac{2\gamma^2(\omega - kv_b \cos\theta)}{1+\gamma^2\theta'^2} \; . \tag{4}$$

In the present Benford setup, $\omega \approx kv_b \approx \omega_p$ and θ is centered at 0, so $\omega' \approx \gamma^2\omega_p\theta^2$. Hence an angular spread in wiggler wave numbers is necessary, and is connected to the broad-band nature of the microwave emission. Thus Compton boosting depends on deviations from a perfect ($\theta = 0$) wiggler, and the geometry is not good for a high-frequency narrow-band microwave generator (of course, the current device was not built to be such a generator, but rather a

simulator of astrophysical processes). To compare with an FEL, the stationary mechanical wiggler has $\theta = \pi$, $\omega = 0$, and $\omega' = 2\gamma^2 kc$. The highest available k for a mechanical wiggler is perhaps 5-6 cm^{-1} which is somewhat less than for the Benford device ($k \approx \omega_p c^{-1} \approx$ 2-20 cm^{-1}). Another important parameter is the wiggler strength. For the mechanical wiggler of an ordinary FEL, the dimensionless wiggler strength is defined as $\epsilon = \Omega_w (kc)^{-1}$, where Ω_w is the cyclotron frequency in the magnetic field of the wiggler; the largest achieved values of ϵ are of order unity. For an electrostatic wiggler, the corresponding strength is $e\phi_L (mc^2)^{-1}$ where $\phi_L = E_L k^{-1}$ is the electrostatic potential. This can also be of order unity, according to (2).

Further theoretical developments are needed in several directions. The first--and hardest--is an understanding of the properties of the fully-saturated electrostatic beam-plasma instability. We have nothing further to offer here, except that numerical simulations of the sort performed for other beam-plasma interactions (Lin, Kaw, and Dawson, 1973; Dawson and Pritchett, private communication, 1982) will be vital.

The second step is to characterize the coherent radiation for a given wiggler configuration (the classic FEL problem). Theorectical approaches of which we are aware are: (1) a purely

phenomenological calculation of the frequency and angular spectrum of the radiation, assumed to come from a coherent group of electrons which have interacted with the wiggler. Such a calculation has been carried out by P. Latham (private communication, 1982) (under the direction of H.A.), and is consistent with the broad-band spectrum seen by Benford. (2) Benford's group is carrying out somewhat more ambitious calculations, which will yield absolutely normalized frequency and power spectra for a given wiggler. These calculations indicate that the necessary fractional coherency (fraction of beam electrons radiating in unison) should be $0(10^{-2} - 10^{-4})$ which translates to $\sim 10^{10}$ electrons in each coherent bunch, a figure roughly consistent with the normalization imposed by Latham. (3) There have been a number of calculations of the properties of an FEL driven by a stationary electrostatic wiggler (Gover, 1979, and references therein). These are especially suited to investigation of possible lasing and power gain in a wave guide or similar cavity where laser action for a small number of modes could take place, but they must be redone for the particular circumstances of a given beam-plasma setup.

Primitive as the present state of theory is, it gives us strong indications of what directions to go in order to make an efficient high-power high-frequency microwave generator. In the first place, the wave numbers of the present Benford device are

hardly larger than those of mechanical FEL wigglers; larger k's mean larger photon frequencies and are thus desirable. In the second place, the present geometry is poor, leading to less-than-maximum Compton boost and large angular spreads, because in (4) $\theta \simeq 0$ and $\omega \simeq kv_b \simeq kc$. The next section shows that a second, slow ion beam can cure both problems.

4.0 A PROPOSED NEW DEVICE

Instead of using the relativistic electron beam both to set up the wiggler and to radiate, let us use a slow ion beam to set up the wiggler (Fig. 5), and then allow the relativistic electrons to scatter from it. The slow beam can have any θ, in particular θ can be near π ($\cos\theta < 0$), thus avoiding one of the defects of the Compton-boosting geometry. More importantly, the wave number of the ion-beam-driven instability which sets up the wiggler can be significantly larger than in the Benford device. This is because in

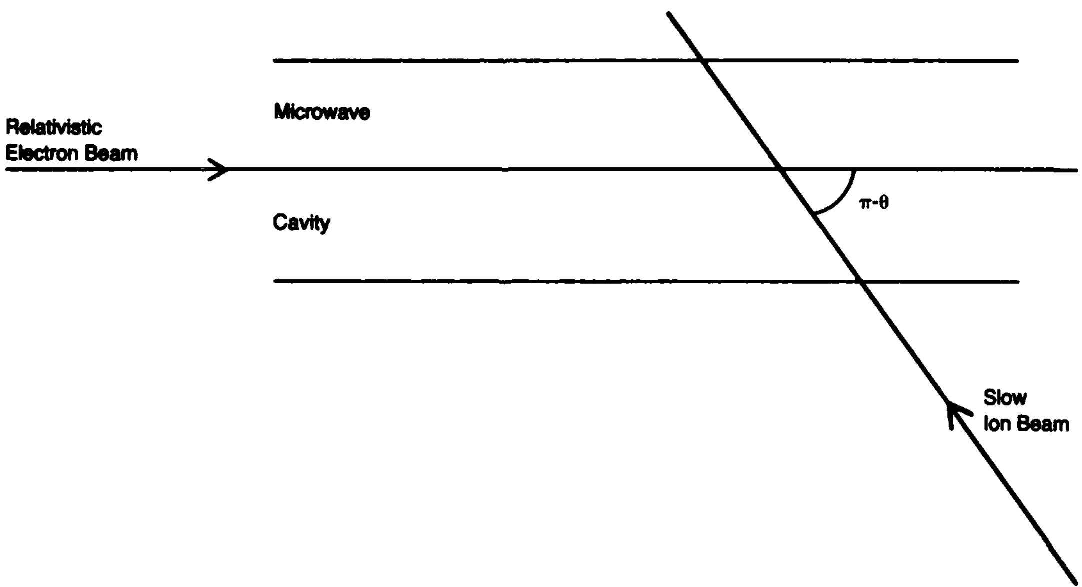

Figure 5. Two-beam microwave generator.

such an instability $k \simeq \omega v_{sb}^{-1}$ (here v_{sb} is the velocity of the slow beam), and while ω is still nearly equal to ω_p, the background plasma frequency, v_{sb} is much less than v_b (the relativistic electron beam velocity). The main limitation on k is that $k\lambda_D < 1$ which turns out to mean that $v_{sb} > \bar{v}_p \simeq 10^8$ cm sec^{-1} where $\bar{v}_p$ is the electron thermal velocity in the background plasma. This requires the ion-beam energy to be greater than 10A keV, where A is the mass number.

We may now rewrite (4) as (ignoring the unimportant denominator)

$$\omega' = 2\gamma^2 \omega_p\left[1 - \cos\theta\left(v_b/v_{sb}\right)\right] . \tag{5}$$

Assume that $\cos\theta \simeq -1$, then for $\omega_p \sim 2 \times 10^{11}$, $\gamma = 3$, $v_b \simeq c$, $v_{sb} = 4 \times 10^8$ (i.e., 100 keV H^+ ions) the Compton-boosted frequency is about 10^{14} Hz (3μ wavelength), well into the infrared. To get such high frequencies we did not depend on deviations from a perfect wiggler, as was necessary in the Benford device, so we are at liberty to try to suppress fluctuations in the spectrum of wiggler wave numbers, or to enhance gain at a selected frequency (tuned cavity), in order to produce a narrow-frequency well-collimated beam of radiation.

So the geometry is good, but what about the coherency of the wiggler? It is not obvious (to us, at least) how to estimate the saturated wiggler strength, because trapping is not the saturation mechanism. The growth time for the beam plasma instability [see (1)] is multiplied by $(M/m)^{1/3}$, where M is the ion mass, and this will still be short compared to the pulse length so the wiggler is still well into the non-linear regime of the instability. Since the ion beam velocity will probably not be enormously larger than the thermal electron velocity, electron heating by Landau damping may be an important saturation process, ultimately leading to coupling with ion-acoustic waves and subsequent ion heating. Clearly, both new experiments and numerical simulations will be necessary; our best hopes are for a wiggler potential which is a finite fraction of the ion energy.

Even though the ion beam is slow, it can carry an enormous amount of energy compared to a relativistic electron beam, because its density can be much greater (up to 10^{15} cm^{-3}). The necessary voltages are relatively low, so uncomplicated devices can be used to generate the beam. Moreover, it is possible to modulate the accelerating voltage at a particular frequency to emphasize this frequency in the wiggler formation process (D. Hammer, private communication). Such modulation is limited by the ion-transit frequency, which might be of the order of 500 MHz.

In a final comparison with an FEL, we might liken the two-beam device to a two-stage FEL. In a two-stage FEL, a mechanical wiggler is used in a first FEL to produce a strong electromagnetic standing wave, which is used as a wiggler for a second FEL. The point is to get wiggler wave numbers much smaller than can be achieved for the mechanical wiggler. No such two-stage FEL has yet been built, but even the most sanguine expectations are for a very weak second-stage wiggler, and very low wall-plug efficiencies. The two-beam device also achieves large wave numbers ($k \simeq \omega_p v_{sb}^{-1} \simeq 500\ \mathrm{cm}^{-1}$), but with wiggler strengths which we expect will be far greater. Moreover, the frequency range from 100's of GHz to the infrared are gotten with electron energies of 1 MeV or so, at power levels which could exceed the already-demonstrated level of MW/GHz broad-band.

5.0 RECOMMENDATIONS

1. Further theoretical analysis of the U.C. Irvine experiment should be pursued.

2. The Irvine experiment should be instrumented for resolving the spectra in the closed windows and for measuring the spectrum to frequencies beyond 120 GHz.

3. Guided by a preliminary idea of applications one should design and build a two beam plasma wiggler FEL as described in this report. Accompanying this should be a serious theoretical effort into the study of the two beam and other plasma wigglers.

4. Numerical simulations should be done of the present Benford device, as well as of the two-beam device, and these "theoretical experiments" should be buttressed by calculations oriented toward the body of theory concerning FELs. Particular attention should be paid to the possibility of achieving lasing or saturated gain in a few modes of a resonating cavity.

5. Evaluation of applications (millimeter-wave radar, jamming device . . .) should be taken up in conjunction with the first two steps.

ACKNOWLEDGMENTS

We thank Greg Benford for many discussions concerning his experiments, Dave Hammer for useful comments on the two-beam device, and Normal Kroll, Bob Novick, and Marshall Rosenbluth for sharing their FEL expertise with use. Also we thank John Dawson and Phil Pritchett for informing us in detail about their numerical simulations of beam-plasma interactions. Finally, we thank Peter Latham for providing us with his analysis of the Benford experiments at U.C. Irvine.

REFERENCES

1. G. Benford, D. Tzach, K. Kato, and D. F. Smith, Phys. Rev. Lett. 45, 1182 (1980).

2. A. Gover, in Free-Electron Generators of Coherent Radiation (ed. S. F. Jacobs et al.), p. 701 (Addison-Wesley, New York, 1979).

3. S. A. Kaplan and V. N. Tsytovich, Plasma Astrophysics (Pergamon, New York, 1973).

4. A. T. Lin, P. K. Kaw, and J. M. Dawson, Phys. Rev. A8 2618 (1973).

5. P. E. Latham, "Intense Electromagnetic Radiation from Collisions of Relativistic Electron Beams with Cold Plasma," preliminary chapters of a PhD dissertation, University of California, Berkeley, June, 1982.

Distribution List

Dr. Henry D.I. Abarbanel, A-005
Scripps Institution of
Oceanography
University of California, S.D.
La Jolla, CA 92093

Dr. Alf Andreassen
Technical Director, OPNAV-095-X
Room 5D616, The Pentagon
Washington, D.C. 20350

Dr. S. Auerback, M Division
Lawrence Livermore National Labs
P.O. Box 808
Livermore, CA 94550

Dr. G. Benford
Department of Physics
University of California, Irvine
Irvine, CA 92717

Dr. Howard E. Brandt (22300)
Harry Diamond Lab.
2800 Powder Mill Road
Adelphi, MD 20783

Dr. Alan Bromborsky (22300)
Harry Diamond Lab.
2800 Powder Mill Road
Adelphi, MD 20783

CDR Paul Brouwer
NFOIO Detachment, Suitland
4301 Suitland Road
Washington, D.C. 20390

Dr. R. Cohen, M Division
Lawrence Livermore National Lab.
P.O. Box 808
Livermore, CA 94550

Dr. Edward E. Conrad
Deputy Director, Science & Tech.
Defense Nuclear Agency
Washington, D.C. 20305

Dr. Robert Cooper [2]
Director, DARPA
1400 Wilson Boulevard
Arlington, VA 22209

Dr. John M. Cornwall
Department of Physics
University of California
Los Angeles, CA 90024

CDR Robert Cronin
Dep Asst Secy Navy (C^3I)
Office of Asst Secy Navy for RE&S
The Pentagon, Room 4E749
Washington, D.C. 20350

Dr. R. Davidson
MIT Plasma Fusion Center
77 Massachusetts Ave. NW16-202
Cambridge, MA 02139

Dr. J. Dawson
Department of Physics
University of California
Los Angeles, CA 90024

Defense Technical Information [2]
Center
Cameron Station
Alexandria, VA 22314

The Honorable Richard DeLauer
Under Secretary of Defense (R&E)
Office of the Secretary of
Defense
The Pentagon, Room 3E1006
Washington, D.C. 20301

Dr. D. DuBois, P Division
Los Alamos National Laboratory
P.O. Box 1663
Los Alamos, NM 87545

Distribution List

Dr. Stanley M. Flatté
1126 Muirlands Vista Way
La Jolla, CA 92037

Director [2]
National Security Agency
Fort Meade, MD 20755
ATTN: Mr. Richard Foss, A052

Mr. Charles A. Fowler, A220
The MITRE Corporation
Bedford Operations
P.O. Box 208
Bedford, MA 01730

Dr. S. William Gouse, W300
The MITRE Corporation
1820 Dolley Madison Blvd.
McLean, VA 22102

Dr. S. Graybill (22900)
Harry Diamond Lab.
2800 Powder Mill Road
Adelphi, MD 20783

Mr. R. Gullickson
DARPA/DEO
1400 Wilson Boulevard
Arlington, VA 22209

Dr. David A. Hammer
109 Orchard Place
Ithaca, NY 14850

Dr. Edward Harper
OPNAV-021T
The Pentagon, Room 4D544
Washington, D.C. 20350

Mr. R. Evan Hineman
P.O. Box 1925
Washington, D.C 20013

The MITRE Corporation [25]
1820 Dolley Madison Blvd.
McLean, VA 22102
ATTN: JASON Library, W002

Mr. John F. Kaufmann
Dep. Dir. for Program Analysis
Office of Energy Research
(ER-31, A1-4000)
U.S. Department of Energy
Washington, D.C. 20545

Dr. George A. Keyworth
Director
Office of Science & Tech. Policy
Executive Office of the President
Washington, D.C. 20500

Mr. Theo Kooij
DARPA
1400 Wilson Boulevard
Arlington, VA 22209

Dr. Norman Kroll
2457 Calle del Oro
La Jolla, CA 92037

Dr. Issai Lefkowitz
Physics Division
Dept. of the Army
U.S. Army Research Office
P.O.B. 12211
Research Triangle Park, NC 27709

Dr. Donald M. LeVine, W385 [3]
The MITRE Corporation
1820 Dolley Madison Blvd.
McLean, VA 22102

Dr. Robert J. Lontz
Director, Physics Division
Dept. of the Army
U.S. Army Research Office
P.O.B. 12211
Research Triangle Park, NC 27709

Distribution List

Dr. Verne L. Lynn
Deputy Director, DARPA
1400 Wilson Boulevard
Arlington, VA 22209

Dr. Gordon MacDonald
The MITRE Corporation
1820 Dolley Madison Blvd.
McLean, VA 22102

Dr. Joseph Mangano [2]
DARPA/DEO
1400 Wilson Boulevard
Arlington, VA 22209

Mr. W. N. Manheimer
Naval Research Lab.
4555 Overlook Ave.
Washington, D.C. 20375

Mr. O. P. Manley
Office of Basic Energy Sciences
ER-15
U.S. Department of Energy
Washington, D.C. 20545

Dr. Claire E. Max, Y Division
Lawrence Livermore National Labs.
P.O. Box 808
Livermore, CA 94550

Mr. John McMahon
Dep. Dir. Cen. Intelligence
Washington, D.C. 20505

Director
National Security Agency
Fort Meade, MD 20755
ATTN: William Mehuron, DDR

Dr. E. Montroll
Department of Physics
Computer Space Sciences Building
Room 3215
University of Maryland
College Park, MD 20742

Dr. Julian Nall [2]
P.O. Box 1925
Washington, D.C. 20013

Director
National Security Agency
Fort Meade, MD 20755
ATTN: Mr. Edward P. Neuburg
DDR-FANX 3

Prof. William A. Nierenberg
Scripps Institution of
Oceanography
University of California, S.D.
La Jolla, CA 92093

Dr. Robert Novick
Astrophysics Laboratory
Columbia University
New York, NY 10027

Dr. T. O'Neil
Department of Physics
University of California, S.D.
La Jolla, CA 92093

Dr. E. Ott
Department of Physics
Energy Research Facility
Room 1202P
University of Maryland
College Park, MD 20742

Dr. Francis W. Perkins, Jr.
Plasma Physics Laboratory
P.O. Box 451
Princeton, NJ 08540

Dr. N. Pierera
Maxwell Labs.
8835 Balboa Avenue
San Diego, CA 92123

Distribution List

Dr. Charles Roberson
Plasma Physics Division
Naval Research Lab.
4555 Overlook Ave.
Washington, D.C. 20375

Mr. Carl Romney
DARPA
1400 Wilson Boulevard
Arlington, VA 22209

Dr. Marshall N. Rosenbluth
University of Texas at Austin
Institute for Fusion Studies,
RLM 11.218
Austin, TX 78712

Dr. Eugene Sevin [2]
Defense Nuclear Agency
Washington, D.C. 20305

ADM William N. Small
Vice Chief of Naval Operations
The Pentagon, Room 4E644
Washington, D.C. 20350

Dr. Joel A. Snow [2]
Senior Technical Advisor
Office of Energy Research
U.S. DOE, M.S. E084
Washington, D.C. 20585

Dr. P. Sprangle
Plasma Physics Division
Naval Research Lab.
4555 Overlook Avenue
Washington, D.C. 20375

Dr. M. Stroscio
Air Force Office of
Scientific Research
B410
Bolling Air Force Base
Washington, D.C. 20332

Mr. Alexander J. Tachmindji, W300
Vice President & General Manager
Washington C^3I Operations
The MITRE Corporation
1820 Dolley Madison Boulevard
McLean, VA 22102

Dr. D. Tanamoto
Maxwell Labs.
8835 Balboa Avenue
San Diego, CA 92123

Dr. Al Trivelpiece
Director, Office of Energy
Research, U.S. DOE
M.S. 6E084
Washington, D.C. 20585

Commander
Naval Surface Weapons Center
ATTN: Dr. H. Uhm, R41
White Oak
Silver Spring, MD 20910

Dr. James P. Wade, Jr.
Prin. Dep. Under Secretary of
Defense for R&E
The Pentagon, Room 3E1014
Washington, D.C. 20301

Maj. Gen. Jasper A. Welch, Jr.
Assistant Deputy Chief of Staff
for Research, Development,
and Acquisition
The Pentagon, Room 4E334
Washington, D.C. 20330

Dr. B. West
La Jolla Institute
P.O. Box 1434
La Jolla, CA 92038

Mr. J. Workman
Berkeley Research Associates
P.O. Box 241
Berkeley, CA 94701

Distribution List

Mr. Leo Young
OUSDRE (R&AT)
The Pentagon, Room 3D1067
Washington, D.C. 20301

Mr. Charles A. Zraket [2]
The MITRE Corporation
P.O. Box 208
Bedford, MA 01730

END

FILMED

4-83

DTIC